



# GRASS GIS Scripts for Satellite Image Analysis by Raster Calculations Using Modules r.mapcalc, d.rgb, r.slope.aspect

Polina Lemenkova

## ► To cite this version:

Polina Lemenkova. GRASS GIS Scripts for Satellite Image Analysis by Raster Calculations Using Modules r.mapcalc, d.rgb, r.slope.aspect. Tehnički vjesnik – Technical Gazette, 2022, 29 (6), pp.1956-1963. 10.17559/tv-20220322091846 . hal-03834515

HAL Id: hal-03834515

<https://hal.science/hal-03834515>

Submitted on 30 Oct 2022

**HAL** is a multi-disciplinary open access archive for the deposit and dissemination of scientific research documents, whether they are published or not. The documents may come from teaching and research institutions in France or abroad, or from public or private research centers.

L'archive ouverte pluridisciplinaire **HAL**, est destinée au dépôt et à la diffusion de documents scientifiques de niveau recherche, publiés ou non, émanant des établissements d'enseignement et de recherche français ou étrangers, des laboratoires publics ou privés.



Distributed under a Creative Commons Attribution - NonCommercial 4.0 International License

# GRASS GIS Scripts for Satellite Image Analysis by Raster Calculations Using Modules `r.mapcalc, d.rgb, r.slope.aspect`

Polina LEMENKOVA

**Abstract:** This study demonstrated the use of GRASS GIS scripts for satellite image analysis. The aim is to perform topographic and environmental analysis in eastern China, Shandong Province, Qingdao region. Variables include land surface temperature evaluated by correlation between the Landsat ETM+ channels and colour composites. The methodology is based on scripting by GRASS GIS modules. Data include two satellite Landsat TM images with a 5 years span (2009 and 2004). The images were imported to GRASS GIS using GDAL library by '`r.in.gdal`' module. The topography (DEM) was assessed by GRASS GIS '`d.rast`' module with isolines plotted using '`r.contour`' and '`d.vect`'. The map elements were displayed by '`v.in.region`', '`d.vect`', '`v.info`'. The slope and aspect maps based on DEM were plotted using module '`r.slope.aspect`' and visualised by a consecutive combination of '`d.rast`', '`r.colours`', '`d.legend`', '`d.text`' and '`d.grid`' modules. The scatterplot of pairwise correlation of the selected Landsat TM7 channels (10 and 20, 50 and 70) was done by '`d.correlate`'. The applied code from the '`r.mapcalc`' was used for image calibration from the DN to apparent radiance at sensor. Two maps showing land surface temperature for 2009 and 2004 were plotted by '`r.mapcalc`'. The land surface temperature maps show lower values over the water and forests, while higher values in cities. Plotting land surface temperature map was made to analyse variations in climate settings in Shandong during 5 years based on the comparative analysis using '`r.mapcalc`' module. The images were plotted by natural and false colour band composites using '`d.rgb`' module and band combinations: 1) colour infrared with focus on vegetation (5-4-3); 2) natural colour composites (1-2-3); 3) contrasting slopes for topography (4-5-7); 4) vegetation analysis (2-3-4); 5) focus on land/water borders (5-6-7). The study has shown cartographic functionality of GRASS GIS scripts specifically for remote sensing data processing and topographic analysis. The environmental modelling has shown variations in land surface temperature, slope steepness and orientation (aspect). The GRASS GIS demonstrated to be an effective tool for remote sensing. Full codes are available on the GitHub repository of the author with provided link to scripts.

**Keywords:** cartography; GRASS GIS; image analysis; mapping; programming; remote sensing; shell script; satellite image

## 1 INTRODUCTION

Recently, remote sensing (RS) data analysis methods which employ techniques of image processing have attracted much interest in cartography. In these methods, it is assumed that a reference dataset consisting of georeferenced images is available. RS data enable to obtain information on objects or areas by measuring their spectral reflectance measured at each pixel cell by GIS. With regard to this, the problem is to derive the information from the target image by techniques of image processing. Multi-temporal satellite images covering the same study area help to map differences in geographic variables: land cover, land surface temperature, land use. There are several known RS data source providers in this context: Landsat TM, SPOT, MODIS, PROBA-V [1], MERIS, SeaWiFS, ENVISAT, ASTER. Various methods proposed algorithms for RS image processing aimed at mapping the environmental changes [2-3].

Current trends in processing RS data using cartographic methods of modelling and visualization present the need to integrate GIS with programming and IT. Such multi-disciplinary approach enables to operate with scripting which can be used to rapidly handle spatial data [4]. The complexity and interdependencies of the environmental system can only be represented and modelled by advanced data analysis which requires algorithms of scripting and automatization [5-8].

Remote sensing data and methods are one of the most important tools in environmental conservation aimed at monitoring ecosystems [9]. The GRASS GIS software (<https://grass.osgeo.org/>) provides a straightforward tool for RS data processing. The abbreviation of GRASS stands for Geographical Resources Analysis Support System. The program enables measuring the complexity of spatial ecosystems and estimating the essential ecological patterns and processes: mapping biodiversity, analysis of forest

structure, retrieval of variables, feature extraction, edge detection and generation of multi-fractal surface as neutral models [10-12]. For example, the '`r.diversity`' module of GRASS GIS enables calculating the landscape diversity using multiple indices at various spatial scales [13].

The repetitive coverage of the Landsat TM images at various time period is vital in change detection applications and models. At the same time, modelling topographic slopes and aspects derived from DEM covering the same study area as satellite image facilitates comparative analysis showing the correlation between variables, e.g., temperature, relief, slope orientation. GRASS GIS is powerful open source software with multiple modules enabling simulation, modelling, visualization, multi-source data analysis (raster, vector, satellite images, digitizing of scanned maps) and pixel-wise computations in a raster map [14]. Existing examples of using GRASS GIS present advanced solutions for cartographic data processing and mapping [15]. The advantages of GRASS GIS consist in the following:

1. **Repeatability:** Scripting enables flexibility and convenience of data processing through full control of commands via command line. Sequential combination of several GRASS GIS modules enables writing shell/bash scripts that can be re-used as templates for similar data processing which is important for repeatability.
2. **Availability:** Open source of the GRASS GIS presents clear advantages over the commercial GIS and handles well the open source data.
3. **Functionality:** Constantly maintained developing of the GRASS GIS presents dozens structured modules enabling various types of data analysis and manipulation in diverse study cases.
4. **Modular structure:** GRASS GIS has a series of modules for satellite image processing, analysis and mapping, which is beneficial for spatial analysis, since RS

based satellite images are the essential data sources for cartography.

Rapid automated data processing by scripts presents important step in cartographic development for advanced data analysis. Although automatization is presented in cartography, there is a constant need for further improvements of the algorithms and methods. Hence, testing scripts is a vital step in development of cartographic methods. Specifically for satellite data processing, e.g., Landsat TM, GRASS GIS has special modules, such as 'i.landsat.acca' and 'i.landsat.toar'. Thus, RS data processing can be performed using numerous GRASS GIS modules specially designed for image processing, as discussed in more details below. The use of GRASS GIS for data processing through shell scripts enables to visualise geographic phenomena, which contributes to our understanding of the geographic processes of the environmental change through technical cartographic support.

Current research presents the application of the modular structure of the GRASS GIS for processing multi-temporal Landsat TM images for environmental analysis. The script-based GRASS GIS approach provides an exceptional opportunity to visualise and model spatial data, and to investigate how environmental parameters vary in space and time. For example, mapping spatial data enables to discover associations between the ecological variables and topography and indicate potential links. For instance, using RS data for modelling and mapping can highlight intensive urbanisation and agricultural activities which reflect the environmental and anthropogenic aspects of land cover changes. Urban areas generally have a higher land surface temperature, while natural land cover types (bare land, forests and water) mostly have lower temperature values. To find out the effect of urbanisation on land cover changes and climate change reflected in land surface temperature, this study used modules of GRASS GIS for processing rasters by scripts.

## 2 APPROACH

### 2.1 Novelty

Scripting techniques has become a state of the art in cartography as an advanced technique for spatial data analysis. However, the applications of scripts, specifically of GRASS GIS, are limited compared to the traditional GUI-based GIS. Even in case of GRASS GIS, it is mostly used for geomorphologic analysis and vector mapping rather than RS image processing. For that purpose, Landsat TM scenes were analysed by GRASS GIS with the aim to demonstrate image analysis using the functionality of GRASS GIS of raster computations.

Since image processing cannot be performed as a single algorithm, several GRASS GIS modules containing different algorithms were employed in the presented workflow: modules r.mapcalc, d.rgb and r.slope.aspect. Whereas using traditional GIS for RS data processing can be well performed, using shell scripts run from the console is a more demanding technique which requires a special attention. This research aims to fill this gap by presenting a case of RS data processing using GRASS GIS. The existing tools of GRASS GIS can be categorised into the two different domains: vector and raster data processing,

according to the type of data structure and formats. This study focuses on raster data. The data are presented by the satellite images Landsat 7.

The objective of this paper is to present a new study on semantic image analysis of Landsat TM scenes by raster calculations in GRASS GIS. Images were used for the environmental analysis: computing land surface temperature and major geomorphological and topographic parameters (slope and aspect) for the area of north-east (NE) China. The study goal was to present an application and usage of modules r.mapcalc, d.rgb and r.slope.aspect of GRASS GIS introduced as scripting approach.

The development of cartography nowadays requires scripting approaches of data processing because of the increasing amount of geospatial open data which rapidly change the demand for information retrieval, speed and accuracy of data analysis. Thus, mapping methods require advanced algorithms to process RS data in a more detailed, rapid, automated and accurate way. This is possible by scripts using GRASS GIS, as presented in this study. Compared to the traditional GIS, scripts have a significant methodological benefit enabling effective data processing. Besides demonstrating scripting algorithms in cartography, this study used the RS data (Landsat images) acquired from the open sources.

### 2.2 Data

The study uses Landsat imagery (Fig. 1). The Landsat mission consisted of several satellites with the Landsat 9 as the most recent one (launched in 2021). The Landsat satellites have various ground track coverage, differing in repeat cycles, swath patterns and Path/Row designators due to the orbital differences.

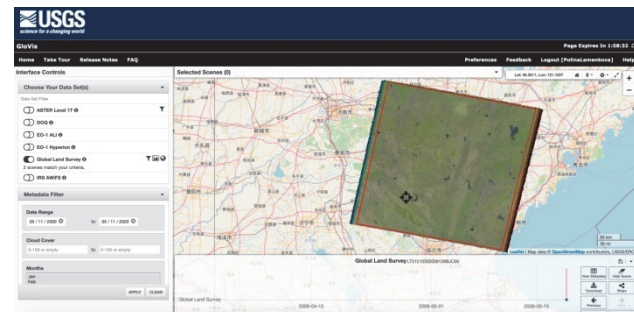


Figure 1 Landsat ETM+ data capture using USGS GloVis

Due to an orbital configuration, Landsat 7 travels from north to south around the Earth and provides the revisit time with an acquisition interval of 16 days which enables repeatability of the coverage in a repeating ground coverage cycle. The Landsat 7 uses the Enhanced Thematic Mapper Plus (ETM+) instrument on board, which is a fixed "whisk-broom", 8-band, multispectral scanning radiometer. By employing the swath technique, Landsat 7 covers an area of 183 km with a 30 m spatial resolution for Bands 1 to 7. This ensures the integrity of the Landsat scenes for cartographic time series analysis and mapping of land cover changes.

The data were acquired by the GloVis USGS and included Landsat images with 5 years span to identify and monitor environmental and topographic parameters in the Shandong Province region, NE China. This study

employed the Landsat ETM+ data from the Landsat 7 satellite mission (Fig. 1). The data include two images taken on different time period with a time span of five years (19 May 2009 and September 10 2004).

### 2.3 Case Study

The images cover eastern region of China, Yellow Sea, Qingdao area, Shandong Province. Shandong is a coastal province of East China region, with a capital of Jinan and major city of Qingdao. It is located on the eastern edge of the North China Plain which covers an area of ca. 409,500 km<sup>2</sup>, most of which is < 50 m a.s.l. The study area is one of the most urbanised and densely populated regions in China. The built environment of the Shandong Peninsula includes strong urbanisation economies, intensive infrastructure development, and processes of urban attraction. These result in high environmental pressure including resource consumption and air pollution. The highest levels of urbanisation in the Shandong Peninsula near Bohai and Yellow Sea include the top three cities with the emergent levels of urban pressure and pollution: Tianjin, Qingdao and Dalian.

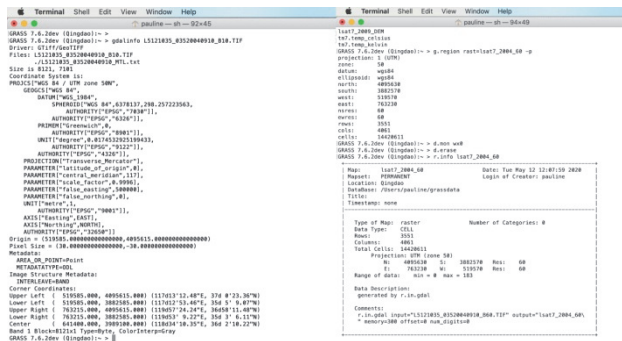


Figure 2 GRASS GIS running 'gdalinfo' utility by GDAL (left) and metadata on Landsat TM image by 'r.info' in GRASS GIS (right). Source: author

Geographically, the Shandong Province of China is represented by the dominated semi and temperate monsoon climate marked with seasonal variations, favourable for planting agricultural areas of different crop types. The agriculture in eastern China includes a wide variety of species on the yellow-soil plains, including, e.g., sorghum, fruits, ornamental plants, vegetables, tobacco, wine, cotton and maize. The environment of eastern China now experiences pressure from agricultural activities, environmental and climate changes.

The topographic and environmental parameters retrieved from the satellite images by GRASS GIS scripts were evaluated and analysed. Specifically, the analysis of terrain curvature, steepness and orientation (slope and aspect) and land surface temperature is presented. All these variables are important parameters for the environmental assessment and agricultural modelling. Among others, land surface temperature is a key indicator in regulation of temperature and surface processes on Earth. Besides, land surface temperature is an important characteristic for energy interchange between the surface and the atmosphere in the cities and tree canopies, as heat waves and thermal balance of an area [16]. Along with vegetation cover and canopy health, land surface temperature is an important indicator of landscape health [17].

```
GRASS 7.6.2dev (Qingdao):> g.list rast
LS121805_052900519_B38
lsat7_2004_09
lsat7_2004_10
lsat7_2004_11
lsat7_2004_12
lsat7_2004_01
lsat7_2004_02
lsat7_2004_03
lsat7_2004_04
lsat7_2004_05
lsat7_2004_06
lsat7_2004_07
lsat7_2004_08
lsat7_2004_09
lsat7_2004_10
lsat7_2004_11
lsat7_2004_12
lsat7_2005_01
lsat7_2005_02
lsat7_2005_03
lsat7_2005_04
lsat7_2005_05
lsat7_2005_06
lsat7_2005_07
lsat7_2005_08
lsat7_2005_09
lsat7_2005_10
lsat7_2005_11
lsat7_2005_12
lsat7_2006_01
lsat7_2006_02
lsat7_2006_03
lsat7_2006_04
lsat7_2006_05
lsat7_2006_06
lsat7_2006_07
lsat7_2006_08
lsat7_2006_09
lsat7_2006_10
lsat7_2006_11
lsat7_2006_12
lsat7_2007_01
lsat7_2007_02
lsat7_2007_03
lsat7_2007_04
lsat7_2007_05
lsat7_2007_06
lsat7_2007_07
lsat7_2007_08
lsat7_2007_09
lsat7_2007_10
lsat7_2007_11
lsat7_2007_12
lsat7_2008_01
lsat7_2008_02
lsat7_2008_03
lsat7_2008_04
lsat7_2008_05
lsat7_2008_06
lsat7_2008_07
lsat7_2008_08
lsat7_2008_09
lsat7_2008_10
lsat7_2008_11
lsat7_2008_12
lsat7_2009_01
lsat7_2009_02
lsat7_2009_03
lsat7_2009_04
lsat7_2009_05
lsat7_2009_06
lsat7_2009_07
lsat7_2009_08
lsat7_2009_09
lsat7_2009_10
lsat7_2009_11
lsat7_2009_12
lsat7_2010_01
lsat7_2010_02
lsat7_2010_03
lsat7_2010_04
lsat7_2010_05
lsat7_2010_06
lsat7_2010_07
lsat7_2010_08
lsat7_2010_09
lsat7_2010_10
lsat7_2010_11
lsat7_2010_12
lsat7_2011_01
lsat7_2011_02
lsat7_2011_03
lsat7_2011_04
lsat7_2011_05
lsat7_2011_06
lsat7_2011_07
lsat7_2011_08
lsat7_2011_09
lsat7_2011_10
lsat7_2011_11
lsat7_2011_12
lsat7_2012_01
lsat7_2012_02
lsat7_2012_03
lsat7_2012_04
lsat7_2012_05
lsat7_2012_06
lsat7_2012_07
lsat7_2012_08
lsat7_2012_09
lsat7_2012_10
lsat7_2012_11
lsat7_2012_12
lsat7_2013_01
lsat7_2013_02
lsat7_2013_03
lsat7_2013_04
lsat7_2013_05
lsat7_2013_06
lsat7_2013_07
lsat7_2013_08
lsat7_2013_09
lsat7_2013_10
lsat7_2013_11
lsat7_2013_12
lsat7_2014_01
lsat7_2014_02
lsat7_2014_03
lsat7_2014_04
lsat7_2014_05
lsat7_2014_06
lsat7_2014_07
lsat7_2014_08
lsat7_2014_09
lsat7_2014_10
lsat7_2014_11
lsat7_2014_12
lsat7_2015_01
lsat7_2015_02
lsat7_2015_03
lsat7_2015_04
lsat7_2015_05
lsat7_2015_06
lsat7_2015_07
lsat7_2015_08
lsat7_2015_09
lsat7_2015_10
lsat7_2015_11
lsat7_2015_12
lsat7_2016_01
lsat7_2016_02
lsat7_2016_03
lsat7_2016_04
lsat7_2016_05
lsat7_2016_06
lsat7_2016_07
lsat7_2016_08
lsat7_2016_09
lsat7_2016_10
lsat7_2016_11
lsat7_2016_12
lsat7_2017_01
lsat7_2017_02
lsat7_2017_03
lsat7_2017_04
lsat7_2017_05
lsat7_2017_06
lsat7_2017_07
lsat7_2017_08
lsat7_2017_09
lsat7_2017_10
lsat7_2017_11
lsat7_2017_12
lsat7_2018_01
lsat7_2018_02
lsat7_2018_03
lsat7_2018_04
lsat7_2018_05
lsat7_2018_06
lsat7_2018_07
lsat7_2018_08
lsat7_2018_09
lsat7_2018_10
lsat7_2018_11
lsat7_2018_12
lsat7_2019_01
lsat7_2019_02
lsat7_2019_03
lsat7_2019_04
lsat7_2019_05
lsat7_2019_06
lsat7_2019_07
lsat7_2019_08
lsat7_2019_09
lsat7_2019_10
lsat7_2019_11
lsat7_2019_12
lsat7_2020_01
lsat7_2020_02
lsat7_2020_03
lsat7_2020_04
lsat7_2020_05
lsat7_2020_06
lsat7_2020_07
lsat7_2020_08
lsat7_2020_09
lsat7_2020_10
lsat7_2020_11
lsat7_2020_12
lsat7_2021_01
lsat7_2021_02
lsat7_2021_03
lsat7_2021_04
lsat7_2021_05
lsat7_2021_06
lsat7_2021_07
lsat7_2021_08
lsat7_2021_09
lsat7_2021_10
lsat7_2021_11
lsat7_2021_12
lsat7_2022_01
lsat7_2022_02
lsat7_2022_03
lsat7_2022_04
lsat7_2022_05
lsat7_2022_06
lsat7_2022_07
lsat7_2022_08
lsat7_2022_09
lsat7_2022_10
lsat7_2022_11
lsat7_2022_12
lsat7_2023_01
lsat7_2023_02
lsat7_2023_03
lsat7_2023_04
lsat7_2023_05
lsat7_2023_06
lsat7_2023_07
lsat7_2023_08
lsat7_2023_09
lsat7_2023_10
lsat7_2023_11
lsat7_2023_12
lsat7_2024_01
lsat7_2024_02
lsat7_2024_03
lsat7_2024_04
lsat7_2024_05
lsat7_2024_06
lsat7_2024_07
lsat7_2024_08
lsat7_2024_09
lsat7_2024_10
lsat7_2024_11
lsat7_2024_12
lsat7_2025_01
lsat7_2025_02
lsat7_2025_03
lsat7_2025_04
lsat7_2025_05
lsat7_2025_06
lsat7_2025_07
lsat7_2025_08
lsat7_2025_09
lsat7_2025_10
lsat7_2025_11
lsat7_2025_12
lsat7_2026_01
lsat7_2026_02
lsat7_2026_03
lsat7_2026_04
lsat7_2026_05
lsat7_2026_06
lsat7_2026_07
lsat7_2026_08
lsat7_2026_09
lsat7_2026_10
lsat7_2026_11
lsat7_2026_12
lsat7_2027_01
lsat7_2027_02
lsat7_2027_03
lsat7_2027_04
lsat7_2027_05
lsat7_2027_06
lsat7_2027_07
lsat7_2027_08
lsat7_2027_09
lsat7_2027_10
lsat7_2027_11
lsat7_2027_12
lsat7_2028_01
lsat7_2028_02
lsat7_2028_03
lsat7_2028_04
lsat7_2028_05
lsat7_2028_06
lsat7_2028_07
lsat7_2028_08
lsat7_2028_09
lsat7_2028_10
lsat7_2028_11
lsat7_2028_12
lsat7_2029_01
lsat7_2029_02
lsat7_2029_03
lsat7_2029_04
lsat7_2029_05
lsat7_2029_06
lsat7_2029_07
lsat7_2029_08
lsat7_2029_09
lsat7_2029_10
lsat7_2029_11
lsat7_2029_12
lsat7_2030_01
lsat7_2030_02
lsat7_2030_03
lsat7_2030_04
lsat7_2030_05
lsat7_2030_06
lsat7_2030_07
lsat7_2030_08
lsat7_2030_09
lsat7_2030_10
lsat7_2030_11
lsat7_2030_12
lsat7_2031_01
lsat7_2031_02
lsat7_2031_03
lsat7_2031_04
lsat7_2031_05
lsat7_2031_06
lsat7_2031_07
lsat7_2031_08
lsat7_2031_09
lsat7_2031_10
lsat7_2031_11
lsat7_2031_12
lsat7_2032_01
lsat7_2032_02
lsat7_2032_03
lsat7_2032_04
lsat7_2032_05
lsat7_2032_06
lsat7_2032_07
lsat7_2032_08
lsat7_2032_09
lsat7_2032_10
lsat7_2032_11
lsat7_2032_12
lsat7_2033_01
lsat7_2033_02
lsat7_2033_03
lsat7_2033_04
lsat7_2033_05
lsat7_2033_06
lsat7_2033_07
lsat7_2033_08
lsat7_2033_09
lsat7_2033_10
lsat7_2033_11
lsat7_2033_12
lsat7_2034_01
lsat7_2034_02
lsat7_2034_03
lsat7_2034_04
lsat7_2034_05
lsat7_2034_06
lsat7_2034_07
lsat7_2034_08
lsat7_2034_09
lsat7_2034_10
lsat7_2034_11
lsat7_2034_12
lsat7_2035_01
lsat7_2035_02
lsat7_2035_03
lsat7_2035_04
lsat7_2035_05
lsat7_2035_06
lsat7_2035_07
lsat7_2035_08
lsat7_2035_09
lsat7_2035_10
lsat7_2035_11
lsat7_2035_12
lsat7_2036_01
lsat7_2036_02
lsat7_2036_03
lsat7_2036_04
lsat7_2036_05
lsat7_2036_06
lsat7_2036_07
lsat7_2036_08
lsat7_2036_09
lsat7_2036_10
lsat7_2036_11
lsat7_2036_12
lsat7_2037_01
lsat7_2037_02
lsat7_2037_03
lsat7_2037_04
lsat7_2037_05
lsat7_2037_06
lsat7_2037_07
lsat7_2037_08
lsat7_2037_09
lsat7_2037_10
lsat7_2037_11
lsat7_2037_12
lsat7_2038_01
lsat7_2038_02
lsat7_2038_03
lsat7_2038_04
lsat7_2038_05
lsat7_2038_06
lsat7_2038_07
lsat7_2038_08
lsat7_2038_09
lsat7_2038_10
lsat7_2038_11
lsat7_2038_12
lsat7_2039_01
lsat7_2039_02
lsat7_2039_03
lsat7_2039_04
lsat7_2039_05
lsat7_2039_06
lsat7_2039_07
lsat7_2039_08
lsat7_2039_09
lsat7_2039_10
lsat7_2039_11
lsat7_2039_12
lsat7_2040_01
lsat7_2040_02
lsat7_2040_03
lsat7_2040_04
lsat7_2040_05
lsat7_2040_06
lsat7_2040_07
lsat7_2040_08
lsat7_2040_09
lsat7_2040_10
lsat7_2040_11
lsat7_2040_12
lsat7_2041_01
lsat7_2041_02
lsat7_2041_03
lsat7_2041_04
lsat7_2041_05
lsat7_2041_06
lsat7_2041_07
lsat7_2041_08
lsat7_2041_09
lsat7_2041_10
lsat7_2041_11
lsat7_2041_12
lsat7_2042_01
lsat7_2042_02
lsat7_2042_03
lsat7_2042_04
lsat7_2042_05
lsat7_2042_06
lsat7_2042_07
lsat7_2042_08
lsat7_2042_09
lsat7_2042_10
lsat7_2042_11
lsat7_2042_12
lsat7_2043_01
lsat7_2043_02
lsat7_2043_03
lsat7_2043_04
lsat7_2043_05
lsat7_2043_06
lsat7_2043_07
lsat7_2043_08
lsat7_2043_09
lsat7_2043_10
lsat7_2043_11
lsat7_2043_12
lsat7_2044_01
lsat7_2044_02
lsat7_2044_03
lsat7_2044_04
lsat7_2044_05
lsat7_2044_06
lsat7_2044_07
lsat7_2044_08
lsat7_2044_09
lsat7_2044_10
lsat7_2044_11
lsat7_2044_12
lsat7_2045_01
lsat7_2045_02
lsat7_2045_03
lsat7_2045_04
lsat7_2045_05
lsat7_2045_06
lsat7_2045_07
lsat7_2045_08
lsat7_2045_09
lsat7_2045_10
lsat7_2045_11
lsat7_2045_12
lsat7_2046_01
lsat7_2046_02
lsat7_2046_03
lsat7_2046_04
lsat7_2046_05
lsat7_2046_06
lsat7_2046_07
lsat7_2046_08
lsat7_2046_09
lsat7_2046_10
lsat7_2046_11
lsat7_2046_12
lsat7_2047_01
lsat7_2047_02
lsat7_2047_03
lsat7_2047_04
lsat7_2047_05
lsat7_2047_06
lsat7_2047_07
lsat7_2047_08
lsat7_2047_09
lsat7_2047_10
lsat7_2047_11
lsat7_2047_12
lsat7_2048_01
lsat7_2048_02
lsat7_2048_03
lsat7_2048_04
lsat7_2048_05
lsat7_2048_06
lsat7_2048_07
lsat7_2048_08
lsat7_2048_09
lsat7_2048_10
lsat7_2048_11
lsat7_2048_12
lsat7_2049_01
lsat7_2049_02
lsat7_2049_03
lsat7_2049_04
lsat7_2049_05
lsat7_2049_06
lsat7_2049_07
lsat7_2049_08
lsat7_2049_09
lsat7_2049_10
lsat7_2049_11
lsat7_2049_12
lsat7_2050_01
lsat7_2050_02
lsat7_2050_03
lsat7_2050_04
lsat7_2050_05
lsat7_2050_06
lsat7_2050_07
lsat7_2050_08
lsat7_2050_09
lsat7_2050_10
lsat7_2050_11
lsat7_2050_12
lsat7_2051_01
lsat7_2051_02
lsat7_2051_03
lsat7_2051_04
lsat7_2051_05
lsat7_2051_06
lsat7_2051_07
lsat7_2051_08
lsat7_2051_09
lsat7_2051_10
lsat7_2051_11
lsat7_2051_12
lsat7_2052_01
lsat7_2052_02
lsat7_2052_03
lsat7_2052_04
lsat7_2052_05
lsat7_2052_06
lsat7_2052_07
lsat7_2052_08
lsat7_2052_09
lsat7_2052_10
lsat7_2052_11
lsat7_2052_12
lsat7_2053_01
lsat7_2053_02
lsat7_2053_03
lsat7_2053_04
lsat7_2053_05
lsat7_2053_06
lsat7_2053_07
lsat7_2053_08
lsat7_2053_09
lsat7_2053_10
lsat7_2053_11
lsat7_2053_12
lsat7_2054_01
lsat7_2054_02
lsat7_2054_03
lsat7_2054_04
lsat7_2054_05
lsat7_2054_06
lsat7_2054_07
lsat7_2054_08
lsat7_2054_09
lsat7_2054_10
lsat7_2054_11
lsat7_2054_12
lsat7_2055_01
lsat7_2055_02
lsat7_2055_03
lsat7_2055_04
lsat7_2055_05
lsat7_2055_06
lsat7_2055_07
lsat7_2055_08
lsat7_2055_09
lsat7_2055_10
lsat7_2055_11
lsat7_2055_12
lsat7_2056_01
lsat7_2056_02
lsat7_2056_03
lsat7_2056_04
lsat7_2056_05
lsat7_2056_06
lsat7_2056_07
lsat7_2056_08
lsat7_2056_09
lsat7_2056_10
lsat7_2056_11
lsat7_2056_12
lsat7_2057_01
lsat7_2057_02
lsat7_2057_03
lsat7_2057_04
lsat7_2057_05
lsat7_2057_06
lsat7_2057_07
lsat7_2057_08
lsat7_2057_09
lsat7_2057_10
lsat7_2057_11
lsat7_2057_12
lsat7_2058_01
lsat7_2058_02
lsat7_2058_03
lsat7_2058_04
lsat7_2058_05
lsat7_2058_06
lsat7_2058_07
lsat7_2058_08
lsat7_2058_09
lsat7_2058_10
lsat7_2058_11
lsat7_2058_12
lsat7_2059_01
lsat7_2059_02
lsat7_2059_03
lsat7_2059_04
lsat7_2059_05
lsat7_2059_06
lsat7_2059_07
lsat7_2059_08
lsat7_2059_09
lsat7_2059_10
lsat7_2059_11
lsat7_2059_12
lsat7_2060_01
lsat7_2060_02
lsat7_2060_03
lsat7_2060_04
lsat7_2060_05
lsat7_2060_06
lsat7_2060_07
lsat7_2060_08
lsat7_2060_09
lsat7_2060_10
lsat7_2060_11
lsat7_2060_12
lsat7_2061_01
lsat7_2061_02
lsat7_2061_03
lsat7_2061_04
lsat7_2061_05
lsat7_2061_06
lsat7_2061_07
lsat7_2061_08
lsat7_2061_09
lsat7_2061_10
lsat7_2061_11
lsat7_2061_12
lsat7_2062_01
lsat7_2062_02
lsat7_2062_03
lsat7_2062_04
lsat7_2062_05
lsat7_2062_06
lsat7_2062_07
lsat7_2062_08
lsat7_2062_09
lsat7_2062_10
lsat7_2062_11
lsat7_2062_12
lsat7_2063_01
lsat7_2063_02
lsat7_2063_03
lsat7_2063_04
lsat7_2063_05
lsat7_2063_06
lsat7_2063_07
lsat7_2063_08
lsat7_2063_09
lsat7_2063_10
lsat7_2063_11
lsat7_2063_12
lsat7_2064_01
lsat7_2064_02
lsat7_2064_03
lsat7_2064_04
lsat7_2064_05
lsat7_2064_06
lsat7_2064_07
lsat7_2064_08
lsat7_2064_09
lsat7_2064_10
lsat7_2064_11
lsat7_2064_12
lsat7_2065_01
lsat7_2065_02
lsat7_2065_03
lsat7_2065_04
lsat7_2065_05
lsat7_2065_06
lsat7_2065_07
lsat7_2065_08
lsat7_2065_09
lsat7_2065_10
lsat7_2065_11
lsat7_2065_12
lsat7_2066_01
lsat7_2066_02
lsat7_2066_03
lsat7_2066_04
lsat7_2066_05
lsat7_2066_06
lsat7_2066_07
lsat7_2066_08
lsat7_2066_09
lsat7_2066_10
lsat7_2066_11
lsat7_2066_12
lsat7_2067_01
lsat7_2067_02
lsat7_2067_03
lsat7_2067_04
lsat7_2067_05
lsat7_2067_06
lsat7_2067_07
lsat7_2067_08
lsat7_2067_09
lsat7_2067_10
lsat7_2067_11
lsat7_2067_12
lsat7_2068_01
lsat7_2068_02
lsat7_2068_03
lsat7_2068_04
lsat7_2068_05
lsat7_2068_06
lsat7_2068_07
lsat7_2068_08
lsat7_2068_09
lsat7_2068_10
lsat7_2068_11
lsat7_2068_12
lsat7_2069_01
lsat7_2069_02
lsat7_2069_03
lsat7_2069_04
lsat7_2069_05
lsat7_2069_06
lsat7_2069_07
lsat7_2069_08
lsat7_2069_09
lsat7_2069_10
lsat7_2069_11
lsat7_2069_12
lsat7_2070_01
lsat7_2070_02
lsat7_2070_03
lsat7_2070_04
lsat7_2070_05
lsat7_2070_06
lsat7_2070_07
lsat7_2070_08
lsat7_2070_09
lsat7_2070_10
lsat7_2070_11
lsat7_2070_12
lsat7_2071_01
lsat7_2071_02
lsat7_2071_03
lsat7_2071_04
lsat7_2071_05
lsat7_2071_06
lsat7_2071_07
lsat7_2071_08
lsat7_2071_09
lsat7_2071_10
lsat7_2071_11
lsat7_2071_12
lsat7_2072_01
lsat7_2072_02
lsat7_2072_03
lsat7_2072_04
lsat7_2072_05
lsat7_2072_06
lsat7_2072_07
lsat7_2072_08
lsat7_2072_09
lsat7_2072_10
lsat7_2072_11
lsat7_2072_12
lsat7_2073_01
lsat7_2073_02
lsat7_2073_03
lsat7_2073_04
lsat7_2073_05
lsat7_2073_06
lsat7_2073_07
lsat7_2073_08
lsat7_2073_09
lsat7_2073_10
lsat7_2073_11
lsat7_2073_12
lsat7_2074_01
ls
```

GRASS GIS project (Fig. 3) after the raster data were listed using module 'g.listrast' and necessary Landsat TM band triplets were selected and visualised using a sequence of the modules (Fig. 3).

Several GRASS GIS modules were used for auxiliary steps. For instance, the 'd.mon' module was used to display the monitor in the GRASS, the 'd.erase' to clean up the previous image on the display, and the 'd.rgb' module for necessary combination of the RGB triplets and their overlay in the active graphical frame. The labels were then added by written expressions as manual annotations using 'd.text' module. This module associates the representation entities, i.e., names and titles on the maps. The resulting combinations of the Landsat TM scenes are visualised in Fig. 4.

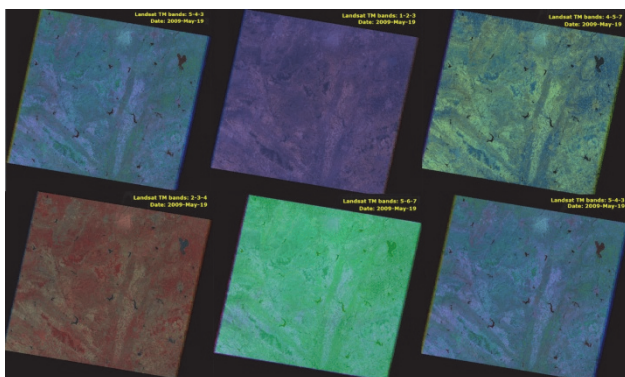


Figure 4 Landsat TM7 band combinations, by GRASS 'd.rgb' module

The topographic mapping is presented on the basis of the available DEM by the GRASS GIS script consisting of several following modules, Fig. 5. The main relief map with 'elevation' colour palette table was plotted by 'd.rast lsat7\_2009\_DEM', Fig. 5.

The isolines were modelled using generic function 'r.contour' of GRASS GIS by 'r.contour lsat7\_2009\_DEM out = Topo\_DEM step = 200 overwrite' command. The contours from a raster map were interpolated at every 200 m interval. The resulted set of vector lines was visualized by GRASS module 'd.vect': d.vectTopo\_DEM colour = 'brown' width = 0, Fig. 5.

The grid was added using command: 'd.grid' w size = 0.5 colour = white border\_colour = yellow width = 0.1 font size = 8 text\_colour = blue bg colour = white', where the size = 0.5 shows the step of the grid. Grid on the map is an important element enabling determination of the coordinates. Therefore, the step of 0.5 was selected and the labels were added with a background to make them distinguishable, Fig. 5.

The border of the region as a thin red line depicting bounding box vector square based on a raster map was added using a sequence of the following commands: v.in.region output = Topo\_DEM\_bbox (here the vector polygon was generated from the region extent); g.listvect (here the list of available vector files was displayed); v.info map = Topo\_DEM\_bbox (the information on the new vector is read); d.vectTopo\_DEM bbox colour = red width = 3 fill\_colour = "none" (f). finally the vector line was added on the map, Fig. 5.

The title (Fig. 1) was added using 'piping' technique: d.title map = lsat7\_2009\_DEM | d.text text = "Topography: Qingdao area" colour = "red" size = 5, followed by 'd.text

text ="DEM" colour = blue size = 2.0 font ="Trebuchet MS".

The DEM data serve for modelling of the topographic variables (slopes), which allows a realistic representation of the Earth's surface. Modelling topographic shapes (Fig. 6) shows steeper and gentler slopes which was used for environmental monitoring. Highly weathered materials and boulders along the valley slopes and high-intensity rainfalls can lead to the hazardous geologic events, such as landslide occurrences in the landforms with steep slopes. The hill-shaded DEM of Qingdao area was used to study the most important geomorphometric parameters, such as slope, aspect of the land surface.

Slope is one of the most important attributes and variables in the landslide analysis and geomorphology. The presence of a slope is a prerequisite for landslide occurrences, because gravitational force tangential to the surface is required to generate the shearing stress.

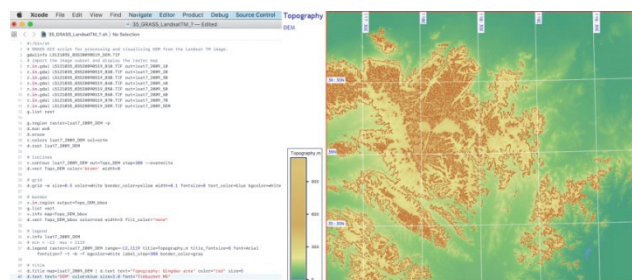


Figure 5 Shell script used for GRASS GIS mapping, visualised in Xcode (left). Topographic map based on DEM, Landsat TM 2009 by GRASS GIS (right)

Steep slopes are prone to landslide occurrences that affect agriculture regions and crops. As can be seen (Fig. 6), the Shandong Province presents various landform types: dissected terrain comprising moderately elevated hills ( $10^{\circ}$  -  $17^{\circ}$ , blue colour), steep slopes ( $17^{\circ}$  -  $45^{\circ}$ , bright purple colour), gentle slopes ( $0^{\circ}$  -  $3^{\circ}$ , light green colour), moderate hills ( $3^{\circ}$  -  $6^{\circ}$ , cyan colour), narrow-deep valleys formed by weathering and erosion of the local river system ( $7^{\circ}$  -  $10^{\circ}$ , light blue coloured areas) flowing eastwards into the Yellow Sea. Following slope modelling, an aspect of the geographical orientation of the compass was plotted (Fig. 6) aimed at visualizing WESN orientation of the slopes in the study area.

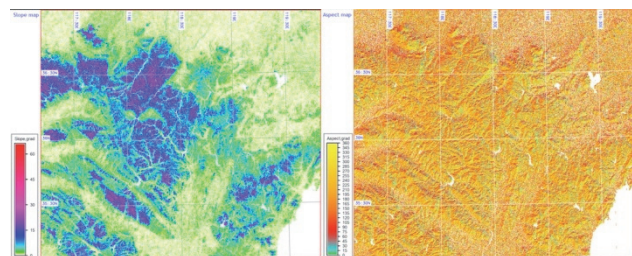


Figure 6 Slope map (left) and aspect map (right) based on DEM, GRASS

Modelling and cartographic visualising of the land surface topography and bathymetry is useful to assess the processes of runoff and erosion which depend on the topographic morphometrics. Modelling slope, aspect, profile curvature and tangential curvature was performed using code: 'r.slope.aspect elevation = lsat7\_2009\_DEM slope = Qslope aspect = Qaspectcurvature =

`Qpcurvtcurvature = Qtcurv'`. Other cartographic elements were plotted by the following code snippets:

- display slope map: `g.region raster = lsat7_2009_DEM -p,`
- display and clean up monitor: `d.mon wx1; d.erase,`
- set up colours: `r.colours-a map = Qslope colour = rainbow,`
- display raster: `d.rastQslope,`
- add legend: `d.legend raster = Qslope title = Slope, gradtitle_fontsize = 8 font = Arial fontsize = 8 -t -b bgcolour = white label_step = 15 border_colour = gray thin = 8,`
- annotate texts: `d.text text = "Slope map" colour = blue size = 3.0 font = "Trebuchet MS",`
- add border: `v.in.region output = Topo_DEM_bbox; g.listvect; v.info map = Topo_DEM_bbox; d.vectTopo_DEM_bbox colour = red width = 3 fill_colour = "none",`
- add grid: `d.grid-w size = 0.5 colour = grey border_colour = yellow width = 0.1 fontsize = 8 text_colour = blue bgcolour = white.`

The majority of the slope orientation has North-East direction (bright orange coloured slopes with  $270^\circ - 360^\circ$ ) followed by North-West direction ( $180^\circ - 270^\circ$ ), Fig. 6. Gentle slopes have a low frequency of landslides due to the lower shear stress associated with low gradients. Hence, contour isolines (200 m) of the topographic map (Fig. 5) were compared with slope and aspect orientation for geomorphometric analysis and the homogeneous unit of the slope angle and aspect was noted (Fig. 6). As channels of the multispectral Landsat TM satellite sensor span a multi-dimensional coordinate system, there is a correlation between the channels for the selected channels of Landsat TM 2009 visualized in Fig. 7.

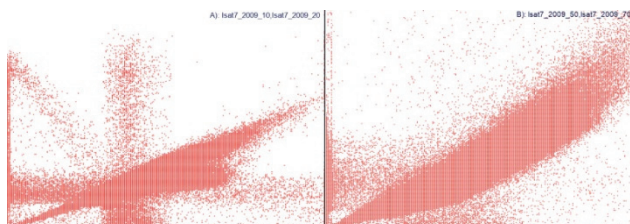


Figure 7 Pairwise correlation scatterplot of two Landsat TM7 channels, plotted using GRASS GIS `d.correlate` module: channels 10 and 20, and 50 and 70

Within this 3D coordinate system, a.k.a. 'feature space' in scripting, each pixel has a certain position depending on the level of brightness in each channel. Respectively, feature space is defined by Landsat TM sensor channels. This position can be presented as a vector in the multi-dimensional coordinate system. Hence, feature space of the two channels was visualized using auxiliary modules: '`d.mon wx0`' and '`d.erase`' for operating with displays. The correlation was visualized by the module '`d.correlate`' used for pairwise correlation in raster: '`d.correlate map = lsat7_2009_10, lsat7_2009_20`' (aerosol and visible blue) and '`d.correlate map = lsat7_2009_50, lsat7_2009_70`' (near-infrared, short wavelength infrared). The '`d.correlate`' module displays correlation between the raster data layers as a scattergram showing results of '`r.stats`' analysis of two rasters (Fig. 7).

The next step included the radiometric preprocessing applied to the raw Landsat TM image. Initially, each pixel showed the apparent radiance measured at the satellite sensor. The initial values were checked from the channel headers using '`r.info`' GRASS module and '`gdalinfo`' by GDAL library. Linear effects were corrected, as pixel values represent a linear transformation of the original data and they needed to fit into range of 8 bit (0 - 255).

Image calibration from the DN to apparent radiance at sensor was done using '`r.mapcalc`' module [19], made by the GRASS GIS code: `r.mapcalc "lsat7_2009_10.rad = ((19.0 - (-6.2))/(255.0 - 1.0)) * (lsat7_2009_10 - 1.0) + (-6.2)"`. This was followed by the inspection of the resulted raster: '`r.info-r lsat7_2009_10.rad`' which gave the following results: `min = -6.2992125984252; max = 19`.

The Landsat-TM7 satellite provides special thermal channel (No. 6) containing thermal information. Therefore, the data delivered by a thermal channel was calibrated to the surface temperature maps (Fig. 8 and Fig. 9). It should be noted that these maps show ground surface temperature, not air temperature. There is an association of the land cover variables with land surface temperature. Surface temperature maps (Fig. 8 for 2009 and Fig. 9 for 2004) were mapped using the channel 6 of the Landsat-TM7 image using '`r.mapcalc`' function.

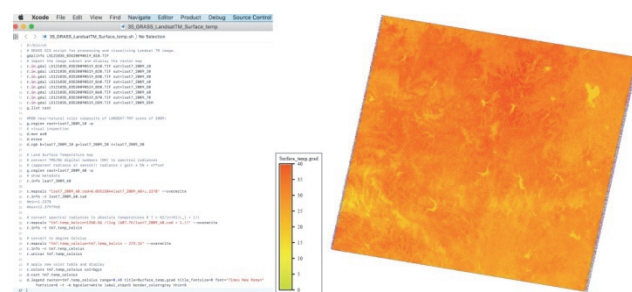


Figure 8 GRASS GIS shell script for mapping (left) and resulting map (right): land surface temperature map for 19.05.2009 by '`r.mapcalc`' GRASS module

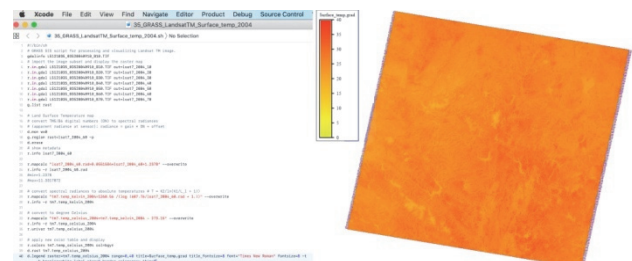


Figure 9 GRASS GIS shell script used for mapping and resulting map: land surface temperature map for 10.09.2004 by '`r.mapcalc`' GRASS GIS module

The calculations applied from the existing algorithms show temperatures (Landsat TM7). These were computed under the assumption of calibration of the physical constants and physical properties of the atmosphere. First, the correction (gain/bias) values were applied to the thermal channel to receive spectral radiances using the existing algorithms. The re-calculated pixel values were converted to the absolute temperature in Kelvin (Fig. 8 and Fig. 9). Third, the results were re-calculated to a degree Celsius temperature map by the '`r.mapcalc`', (Fig. 8 and Fig. 9).

The resulting land surface temperature maps (Fig. 8 and Fig. 9), show the average land surface temperature in Celsius degrees with a range of pixels with lower

temperatures (water areas in lakes and forests) and higher temperatures (urban areas). A yellow-to-red colour table was applied for the visualised map for the 19 May 2009 and 10 September 2004. This map shows the distributed emitted thermal radiation in degree Celsius in general colour scale for positive temperatures from 0° to 40°.

The practical application of GRASS GIS is demonstrated in this paper by a case study of Landsat TM images processing using GRASS GIS scripts.

#### 4 RESULTS AND DISCUSSION

The presented research benefited from the GRASS GIS modular architecture, since multiple models were integrated into a single script for plotting maps (Fig. 1 to Fig. 9). The results of satellite image processing showed natural and false colour composites in vegetation and urban areas plotted by 'd.rgb' module of GRASS GIS. Following combinations were visualized: 1) colour infrared with focus on vegetation (bands 5-4-3); 2) natural colour composites (bands 1-2-3); 3) contrasting slopes for topography (bands 4-5-7); 4) vegetation analysis (bands 2-3-4); 5) focus on land/water borders (bands 5-6-7). The environmental parameters of the study area show high correspondence with topographic situation and land use types: land surface temperature has lower values over water areas and forests, while higher values in urban areas. Notable changes in land surface temperature are detected during the assessed time span, from 2004 to 2009 seasons. This points at gradually increased urbanisation in this area. Changes in land surface temperature and geomorphic parameters (slope, aspect) were quantified using a set of the GRASS GIS modules.

Technical flexibility of GRASS GIS is demonstrated by four case studies: 1) colour composites; 2) topographic DEM visualization and modelling its derivatives (slope and aspect); 3) plotting correlation of spectral channels; 4) modelling land surface temperature based on the Landsat TM Band short-wave Infrared (SWIR) 6 with wavelengths of 10.40 - 12.50 μm and with 30 m spatial resolution.

Using GRASS GIS, several scripts applying modules for raster data processing were applied and output maps visualised (Fig. 5, Fig. 8 and Fig. 9). GRASS GIS console was used for implementing modules (Fig. 2 and Fig. 3). The cartographic framework of our workflow included several steps. First, the colour composites were generated using extraction of features in various bands on Landsat TM image. The elevation based on DEM modelling enabled to query the derivatives, such as slope and aspect. Next, the correlation of spectral channels was analysed and the variations searched. Finally, land surface temperature was modelled and visualized based on the SWIR 6 band. All the steps were performed using scripts which employ a robust GRASS GIS syntax for data processing and computing. This is particularly essential for processing a time series of images which should be analysed in the identical standardized way. Unlike the traditional GIS mapping, using scripts performs fast and accurate, which presents one of the strongest advantages of script-based geospatial analysis.

The results show correlation in spatio-temporal change of land surface temperature and topographic elevations which demonstrated different patterns over urbanised areas

(cities) and natural areas (forests, bare lands and water). This proved that land cover changes derived from the satellite images can be a useful indicator for environmental monitoring. Besides the environmental aspects, this study also pointed at technical aspects of the GRASS GIS and presented modules used in a combined way for cartographic data processing by scripts.

The Global Visualization Viewer (GloVis) by USGS was used for downloading Landsat TM images through selecting study area by coordinates, viewing metadata and image capture. Presented application of GRASS GIS data analysis aims to comparatively overlay raster maps visualising models from multiple domains: topography and geomorphology (Fig. 5 and Fig. 6), environment and climate change (Fig. 8 and Fig. 9) as well as RS data and technical aspects of Landsat TM bands (Fig. 4 and Fig. 7). Besides the integration of GIS and IT, GRASS GIS scripting technique aims at advanced geospatial analysis.

This paper demonstrated the functionality of GRASS GIS as an excellent cartographic tool for spatial modelling. It includes a wide variety of tasks: raster data conversion and importing, geodetic warping and re-projection, statistical analysis, geomorphometric analysis and modelling, design, visualisation, project management. The integrated use of DEM, satellite images and GRASS approach provided important approach for environmental evaluation in eastern China.

Visualization of the slope and aspect settings enables to show level of landform borders (horst, grabens as main landforms). Mapping slope gradient and its derivatives (profile and tangential curvature, aspect) can be used for modelling hierarchical landforms classifications. The importance of the geomorphic modelling consists in fundamental nature of the relief, which shows vertical dissection of the terrain. The RS based mapping is used to highlight the geomorphological features on the surfaces by means of image processing. Hence, the interpretative cartographic visualization uses instrumental observations for thematic mapping based on spatio-temporal sensor observations [20]. Slope steepness amplitude of the terrain dissection, correlated with geomorphological development, is strongly affected by geologic processes.

#### 5 CONCLUSIONS

This study presented an advanced scripting approach of GRASS GIS that enables processing spatial datasets by scripts from the console without GUI. Full scripts are provided in the GitHub repository of the author with shared link to the codes. The goal of cartographic data processing is to reduce time and labour workflow and to increase the level of automation for accurate and rapid data processing. The RS requires increased automation to obtain the objective results in data modelling and classification. As a response to these needs, GRASS GIS presents advantageous techniques in many aspects, as follows:

- GRASS GIS shell scripting technique run from console enables to repeat scripts. Once written, scripts can be repeated and applied to process similar data. Thus, the biggest advantage of scripts consists in repeatability.
- GRASS GIS has relevant modules specially designed for image processing: 'd.rast', 'r.colours', 'r.mapcalc', 'd.rgb'. Special modules can be used for vector data

processing and data reading ('v.in.region', 'd.vect', 'v.info' and 'r.in.gdal'). Thus, another advantage is flexibility of data formats and processing.

- The environmental analysis was done using RS data based on the information derived from the satellite images. Therefore, it can be extended to many fields in applications in similar environmental or urban studies using the Landsat TM/ETM+ images. Thus, another advantage of the GRASS GIS can be formulated as broad thematic applications, such as urban mapping, environmental analysis, etc.

The GRASS GIS demonstrated in this paper proved to be effective GIS with functionality for processing raster Landsat TM images through scripting approach. Besides the cartographic functionality, GRASS GIS has strong technical advantages, since its supporting modules are available for many operating systems (MacOS, Windows, Linux). Furthermore, GRASS GIS functionality can be accessed through a Python and R language interface widely used in geosciences [21-24] making it possible to integrate programming in tasks of geospatial analysis, including image processing.

Because GRASS GIS is an open source software, its developing is being constantly improved, fixed, and customized for creating new modules for vector and raster data processing. GRASS GIS supports a variety of formats, some of which are native to its executable, while others accessed through GDAL/OGR libraries via 'r.in.gdal'. This enables to import data directly into GRASS GIS. GDAL libraries add an extra level of communication between the GRASS GIS and data sources and increase flexibility of data processing.

Since many GIS benefit from the integrated and multi-source data processing for modelling and visualization of modeled geographic phenomena through satellite image analysis (Landsat TN, MODIS, ASTER, Pleiades, Sentinel-2), integrating modules for distributed data analysis through scripts is increasingly useful.

There are multiple ways of scripting integration in cartography, from adhering to plugins directly to GIS, e.g., Python plugin at QGIS, to developing console based structure, e.g., GMT. The advantages of scripts in programming and GIS consist in their repeatability. Scripting ensures achieving a reusable approach in cartography, as scripts are applicable for data reprocessing, e.g. using them as templates for processing other datasets. However, a multi-disciplinary approach in GIS combining shell scripting and spatial analysis is a challenge, as this requires a user to have a background in programming and requires skills in shell scripting and understanding of logic and principles of data analysis, which can support GIS at the advanced level.

As a contribution to the development of cartographic research at advanced level, this paper presented the use of GRASS GIS and a GDAL library for thematic processing of the Landsat TM images. Several scripts are included as Xcode screenshots and full codes are available in the GitHub repository. GRASS GIS console print screens are shown as illustrations and workflow explained stepwise and the resulting map for illustration of the approach. The GRASS GIS supports both GUI and console-based data processing. Besides, it is employing modular architecture where models are designed for vector and raster data

processing and visualization, instead of the direct manipulation with data as in GUI-based GIS [25-27].

As demonstrated, scripts of GRASS GIS were used to analyse satellite images, to do calculations by 'r.mapcalc' module and to demonstrate variations in land surface temperature. Several colour composites were tested by the 'd.rgb' GRASS GIS module and shown to demonstrate usability of Landsat TM images for land/water analysis (distinguishability, land cover types and topographic surface mapping). This research contributed both to the technical development of script-based cartographic methods and to the regional studies of China.

## Acknowledgements

The author is thankful to the two anonymous reviewers and Editors for their critical comments and suggestions on this paper which improved the initial version of the text.

## 6 REFERENCES

- [1] Abdramane, D., Ye, X., & Amadou, T. (2018). Analysis of Land surface Temperature change based on MODIS data, Case study: Inner Delta of Niger. *Natural Hazards and Earth System Sciences*, 2018, 1-20. <https://doi.org/10.5194/nhess-2018-208>
- [2] Adrian, J., Sagan, V., & Maimaitijiang, M. (2021). Sentinel SAR-optical fusion for crop type mapping using deep learning and Google Earth Engine. *ISPRS Journal of Photogrammetry and Remote Sensing*, 175, 215-235. <https://doi.org/10.1016/j.isprsjprs.2021.02.018>
- [3] Akinbobola, A. (2019). Simulating Land Cover Changes and Their Impacts on Land Surface Temperature in Onitsha, South East Nigeria. *Atmospheric and Climate Sciences*, 9, 243-263. <https://doi.org/10.4236/acs.2019.92017>
- [4] Bhattacharyya, B. K. & Holroyd, M. R. (1971). Numerical Treatment and Automatic Mapping of Two-Dimensional Data in Digital Form. *Proceedings of 9th International Symposium of Techniques for Decision-Making in the Mineral Industry*, 12, 148-158.
- [5] Cavallo, A. & Norese, M. F. (2001). GIS and Multicriteria Analysis to Evaluate and Map Erosion and Landslide Hazards. *Informatica*, 12(1), 25-44.
- [6] Dash, P., Götsche, F. M., Olesen, F. S., & Fischer, H. (2002). Land Surface Temperature and Emissivity Estimation from Passive Sensor Data: Theory and Practice-Current Trends. *International Journal of Remote Sensing*, 23, 2563-2594. <https://doi.org/10.1080/01431160110115041>
- [7] Barbierato, E., Bernetti, I., Capecchi, I., & Saragosa, C. (2019). Quantifying the impact of trees on land surface temperature: A downscaling algorithm at city-scale. *European Journal of Remote Sensing*, 52, 74-83. <https://doi.org/10.1080/22797254.2019.1646104>
- [8] Cook, M., Schott, J. R., Mandel, J., & Raqueno, N. (2014). Development of an Operational Calibration Methodology for the Landsat Thermal Data Archive and Initial Testing of the Atmospheric Compensation Component of a Land Surface Temperature (LST) Product from the Archive. *Remote Sensing*, 6(11), 11244-11266. <https://doi.org/10.3390/rs61111244>
- [9] Fang, X., Shi, X., & Gao, W. (2021). Measuring urban sustainability from the quality of the built environment and pressure on the natural environment in China: A case study of the Shandong Peninsula region. *Journal of Cleaner Production*, 289, 125-145. <https://doi.org/10.1016/j.jclepro.2020.125145>

- [10] Lemenkova, P. (2020). GRASS GIS for topographic and geophysical mapping of the Peru-Chile Trench. *Forum geografic*, 19, 143-157. <https://doi.org/10.5775/fg.2020.009.d>
- [11] Fensholt, R., Sandholt, I., & Rasmussen, M. S. (2004). Evaluation of MODIS LAI, fAPAR and the relationship between fAPAR and NDVI in a semi-arid environment using in situ measurements. *Remote Sensing of Environment*, 91, 490-507. <https://doi.org/10.1016/j.rse.2004.04.009>
- [12] Lemenkova, P. (2021). Dataset compilation by GRASS GIS for thematic mapping of Antarctica: Topographic surface, ice thickness, subglacial bed elevation and sediment thickness. *Czech Polar Reports*, 11, 67-85. <https://doi.org/10.5817/CPR2021-1-6>
- [13] Rocchini, D., Delucchi, L., Bacaro, G., Cavallini, P., Feilhauer, H., Foody, G. M., He, K. S., Nagendra, H., Porta, C., Ricotta, C., Schmidlein, S., Spano, L. D., Wegmann, M., & Neteler, M. (2013). Calculating landscape diversity with information-theory based indices: A grass gis solution. *Ecological Informatics*, 17, 82-93. <https://doi.org/10.1016/j.ecoinf.2012.04.002>
- [14] Neteler, M. & Mitasova, H. (2008). *Open Source GIS: A GRASS GIS Approach*. Springer Science+Business Media, LLC, Berlin. <https://doi.org/10.1007/978-0-387-68574-8>
- [15] Andreo, V., Dogliotti, A. I., Tauro, C., & Neteler, M. (2015). Spatio-temporal variations in chlorophyll-a concentration in the patagonic continental shelf: An example of satellite time series processing with GRASS GIS temporal modules. *2015 IEEE International Geoscience and Remote Sensing Symposium (IGARSS)*, 2249-2252. <https://doi.org/10.1109/IGARSS.2015.7326254>
- [16] Jung, M. C., Dyson, K., & Alberti, M. (2021). Urban Landscape Heterogeneity Influences the Relationship between Tree Canopy and Land Surface Temperature. *Urban Forestry & Urban Greening*, 57, 126930. <https://doi.org/10.1016/j.ufug.2020.126930>
- [17] Jamali, A. A., Ghorbani Kalkhajeh, R., Randhir, T. O., & He, S. (2022). Modeling relationship between land surface temperature anomaly and environmental factors using GEE and Giovanni. *Journal of Environmental Management*, 302, 113970. <https://doi.org/10.1016/j.jenvman.2021.113970>
- [18] Xiao, J., Shen, Y., Ge, J., Tateishi, R., Tang, C., Liang, Y., & Huang, Z. (2006). Evaluating urban expansion and land use change in Shijiazhuang, China, by using GIS and remote sensing. *Landscape and Urban Planning*, 75(1), 69-80. <https://doi.org/10.1016/j.landurbplan.2004.12.005>
- [19] Shapiro, M. & Westervelt, J. (1992). *r.mapcalc. An algebra for GIS and image processing*. Technical report, US-Army CERL.
- [20] Frigeri, A., Hare, T., Neteler, M., Coradini, A., Federico, C., & Orosei, R. (2011). A working environment for digital planetary data processing and mapping using ISIS and GRASS GIS. *Planetary and Space Science*, 59(11), 1265-1272. <https://doi.org/10.1016/j.pss.2010.12.008>
- [21] Lemenkova, P. (2019). Statistical Analysis of the Mariana Trench Geomorphology Using R Programming Language. *Geodesy and Cartography*, 45, 57-84. <https://doi.org/10.3846/gac.2019.3785>
- [22] White, J. T., Fienen, M. N., & Doherty, J. E. (2016). A Python framework for environmental model uncertainty analysis. *Environmental Modelling & Software*, 85, 217-228. <https://doi.org/10.1016/j.envsoft.2016.08.017>
- [23] Knox, S., Meier, P., Yoon, J., & Harou, J. J. (2018). A Python framework for multi-agent simulation of networked resource systems. *Environmental Modelling & Software*, 103, 16-28. <https://doi.org/10.1016/j.envsoft.2018.01.019>
- [24] Lemenkova, P. (2019). Testing Linear Regressions by StatsModel Library of Python for Oceanological Data Interpretation. *Aquatic Sciences and Engineering*, 34, 51-60. <https://doi.org/10.26650/ASE2019547010>
- [25] Fu, P. & Weng, Q. (2016). A time series analysis of urbanization induced land use and land cover change and its impact on land surface temperature with Landsat imagery. *Remote Sensing of Environment*, 175, 205-214. <https://doi.org/10.1016/j.rse.2015.12.040>
- [26] Hulley, G. C., Hughes, C. G., & Hook, S. J. (2012). Quantifying uncertainties in land surface temperature and emissivity retrievals from ASTER and MODIS thermal infrared data. *Journal of Geophysical Research: Atmospheres*, 117(D23). <https://doi.org/10.1029/2012JD018506>
- [27] Toté, C., Swinnen, E., Sterckx, S., Clarijs, D., Quang, C., & Maes, R. (2017). Evaluation of the SPOT/VEGETATION Collection 3 reprocessed dataset: Surface reflectances and NDVI. *Remote Sensing of Environment*, 201, 219-233. <https://doi.org/10.1016/j.rse.2017.09.010>

#### Contact information:

**Polina LEMENKOVA**

Université Libre de Bruxelles,  
École polytechnique de Bruxelles (EPB, Brussels Faculty of Engineering),  
Laboratory of Image Synthesis and Analysis,  
Campus de Solbosch, ULB-LISA CP165/57,  
Avenue Franklin D. Roosevelt 50, B-1050 Brussels, Belgium  
E-mail: polina.lemenkova@ulb.be